Cancer Chemother Pharmacol (2011) 67:265–273
DOI 10.1007/s00280-010-1314-0

ORIGINAL ARTICLE

In vitro anti-mesothelioma activity of cisplatin–gemcitabine combinations: evidence for sequence-dependent effects

Ilaria Zanellato · Carla Doriana Boidi · Guido Lingua · Pier-Giacomo Betta · Sara Orecchia · Elena Monti · Domenico Osella

Received: 16 December 2009 / Accepted: 19 March 2010 / Published online: 6 April 2010

Abstract
Purpose The present study addresses the optimization of gemcitabine–cisplatin protocols currently adopted in the clinical management of malignant pleural mesothelioma (MPM), using cell lines derived from different histological subtypes of MPM as an in vitro model.
Methods MPM cell lines were exposed either to single drugs or to their combinations, using a fixed dose ratio. Possible mechanisms for synergistic interactions were investigated by cell cycle analysis, western blot analysis of p53 phosphorylation status, and neutral comet assay to detect double strand breaks.
Results Four-hour pre-treatment with gemcitabine followed by 68-h exposure to cisplatin was found to exert synergistic activity in both epithelioid and sarcomatoid MPM subtypes, inducing a strong S-phase arrest that correlated with accumulation of double-strand breaks (DSBs).
Conclusion The antiproliferative effects of the gemcitabine/cisplatin combination in mesothelioma cells can be maximized by pre-treatment with gemcitabine, suggesting that this drug increases cisplatin-induced DSBs by inhibiting DNA adduct repair.

Keywords Malignant pleural mesothelioma · Cisplatin · Gemcitabine · Combination chemotherapy

Electronic supplementary material The online version of this article (doi:10.1007/s00280-010-1314-0) contains supplementary material, which is available to authorized users.

I. Zanellato · C. D. Boidi · G. Lingua · D. Osella (✉)
Department of Environmental and Life Sciences,
Università del Piemonte Orientale "Amedeo Avogadro",
Via T. Michel, 11, 15121 Alessandria, Italy
e-mail: domenico.osella@mfn.unipmn.it

P.-G. Betta · S. Orecchia
Pathology Unit, Department of Oncology,
Azienda Sanitaria Ospedaliera, Via Venezia 16,
15121 Alessandria, Italy

E. Monti
Department of Structural and Functional Biology,
Section of Pharmacology, University of Insubria,
Via A. da Giussano 12, 21052 Busto Arsizio, Italy

Introduction

Malignant pleural mesothelioma (MPM) is a lethal tumour primarily associated with previous asbestos exposure. In spite of the ban issued during the last 15 years by most western countries against asbestos use and production, the incidence of MPM is on the rise and expected to peak around 2012 due to previous widespread asbestos consumption, and to the long latency period (20–30 years) elapsing between exposure and clinical presentation of the disease. In addition, countries like China and Russia continue to produce and use large amounts of asbestos, the full consequences of which will only become apparent in a few decades. Addressing the global health problem presented by asbestos-induced MPMs is complicated by difficulties in early diagnosis of the disease, as no reliable biological markers are currently available for the screening of asbestos-exposed populations, and the onset of MPM is usually non-specific, insidious, and followed by rapid progression of the disease within a few months. As a result, the vast majority of MPM patients are diagnosed with locally advanced unresectable disease, which results in a median survival time of only 9.8 months [1]. Chemotherapy is currently the only treatment option for most patients diagnosed at this late stage, as few patients are suitable for radical

surgery, while radiotherapy can only alleviate symptoms without affecting overall survival. In 2002, an extensive meta-analysis indicated cisplatin (*cis*-diamminedichloroplatinum (II), CDDP) as the most effective single agent for MPM treatment, in spite of an objective response rate of only 23% and of the accompanying side toxicities [2]. Since then, combinations of platinum derivatives with newer agents, such as pemetrexed and gemcitabine, have considerably broadened the spectrum of therapeutic options [3], yielding response rates of 41% for cisplatin/pemetrexed [4] and from 12 to 73% for cisplatin/gemcitabine [5, 6]. Importantly, both combinations were associated with improved lung function and global quality of life, and with a low rate of disease progression. Cisplatin/gemcitabine combinations have been extensively evaluated both in vitro and in vivo in several tumour types, including head/neck and ovarian carcinomas and non-small cell lung cancers (NSCLC), showing antagonistic, additive, or synergistic effects, depending on the tumour type and treatment schedule [7, 8]; however, the effects of the combination on MPM cell lines have not yet been reported.

The primary aim of this study was to optimize the efficacy of cisplatin–gemcitabine combinations by evaluating possible sequence-dependent effects, using cell lines of comparatively recent derivation from human MPM effusions. We also developed a variant MPM cell line selected from the parental sarcomatoid MM98 cell line by continuous exposure to cisplatin, which was used to assess the ability of gemcitabine to overcome cisplatin resistance. A secondary aim of the study was determine whether tumour histology significantly affected MPM cell response to the combination and/or its dependence on the drug sequence adopted. In fact, MPMs can broadly be classified into three basic histological types, namely epithelioid (the most common), sarcomatoid, and mixed [9]: differences in the genetic makeup of epithelioid and sarcomatoid MPMs may contribute to the observed variability in clinical behaviour and response to treatment in this tumour type.

Materials and methods

Cell lines

Four cell lines derived from pleural effusions of untreated MPM patients were used: BR95 [10] and MM98 [11, 12] were used between passages 20 and 40, and two newly established lines, MG06 and DE05 were used between passages 5 and 15. Histologically, BR95 and MG06 cells were originally derived from epithelioid tumours, whereas MM98 cells originated from a sarcomatoid and DE05 from a mixed or biphasic type (with an epithelioid component of approximately 80%) tumour. All the patients came from the same geographic area, where residual environmental pollution from a large asbestos factory, that had been active for over 60 years, is still detectable. Cells were grown in Ham's F10 medium (Gibco, Invitrogen Life Science, S. Giuliano Milanese, Italy and Sigma–Aldrich, St. Louis, MO, USA) supplemented with L-glutamine (4 mM, Gibco), penicillin (100 IU/ml, Gibco), streptomycin (100 g, Gibco), and 10% foetal bovine serum (Gibco). BR95, MG06, and DE05 cells showed polygonal and epithelial-like morphology, whereas MM98 showed spindle-like morphology. Population doubling times were 28, 20, 24, and 48 h for BR95, MM98, MG06, and DE05, respectively.

Drug preparation and cell treatment

Cisplatin (Sigma) and gemcitabine (Eli Lilly) were dissolved in 0.9% NaCl and sterile filtered. Aqueous HCl was added to the cisplatin stock solution (0.5 mM) up to pH 3, in order to avoid hydrolysis during storage at −80°C. For single-drug experiments, two different protocols were adopted: (1) 72-h continuous treatment (CT) and (2) 4-h treatment (T), followed by drug wash-out with PBS and 68-h recovery (R) in fresh medium. Combination experiments were carried out using fixed dose ratios [13]. For simultaneous administration, a stock solution containing the two drugs at their respective IC_{50} values was prepared and serially diluted, down to three orders of magnitude lower. To study sequence-dependent effects, cells were treated for 4 h with the first drug (T), at concentrations ranging from its IC_{50} down to three orders of magnitude lower, washed with PBS, and then treated for 68 h (CT) with concentrations of the second drug, also ranging from its IC_{50} to three orders of magnitude lower, using the same dilution ratios for both drugs. A representative scheme of drug treatment schedules is depicted in Fig. 1a.

Cell viability and apoptosis

MPM cells (1×10^4–2×10^4 cells/well) were seeded onto 96-well flat-bottom plates and allowed to attach 24 h before drug treatment. At the end of the experiment, the [3-(4, 5-dimethylthiazol-2-yl)-5-(3-carboxymethoxyphenyl)-2-(4-sulfophenyl)-2H-tetrazolium], inner salt (MTS) assay was performed using a commercial kit (CellTiter Aqueous Solution, Promega), according to the manufacturer's instructions; absorbance values were recorded at 490/620 nm by a spectrophotometric plate reader (Sirio S, SEAC, Florence, Italy) and corrected by subtraction of the absorbance of MTS alone. For the ATP-CSA (Chemo Sensitivity Assay) [14], 2×10^3–3×10^3 cells/well were plated onto white-wall 96-well microtitre plates (cell culture-treated, Optilux, BD Biosciences) 24 h before treatment and exposed to cis-

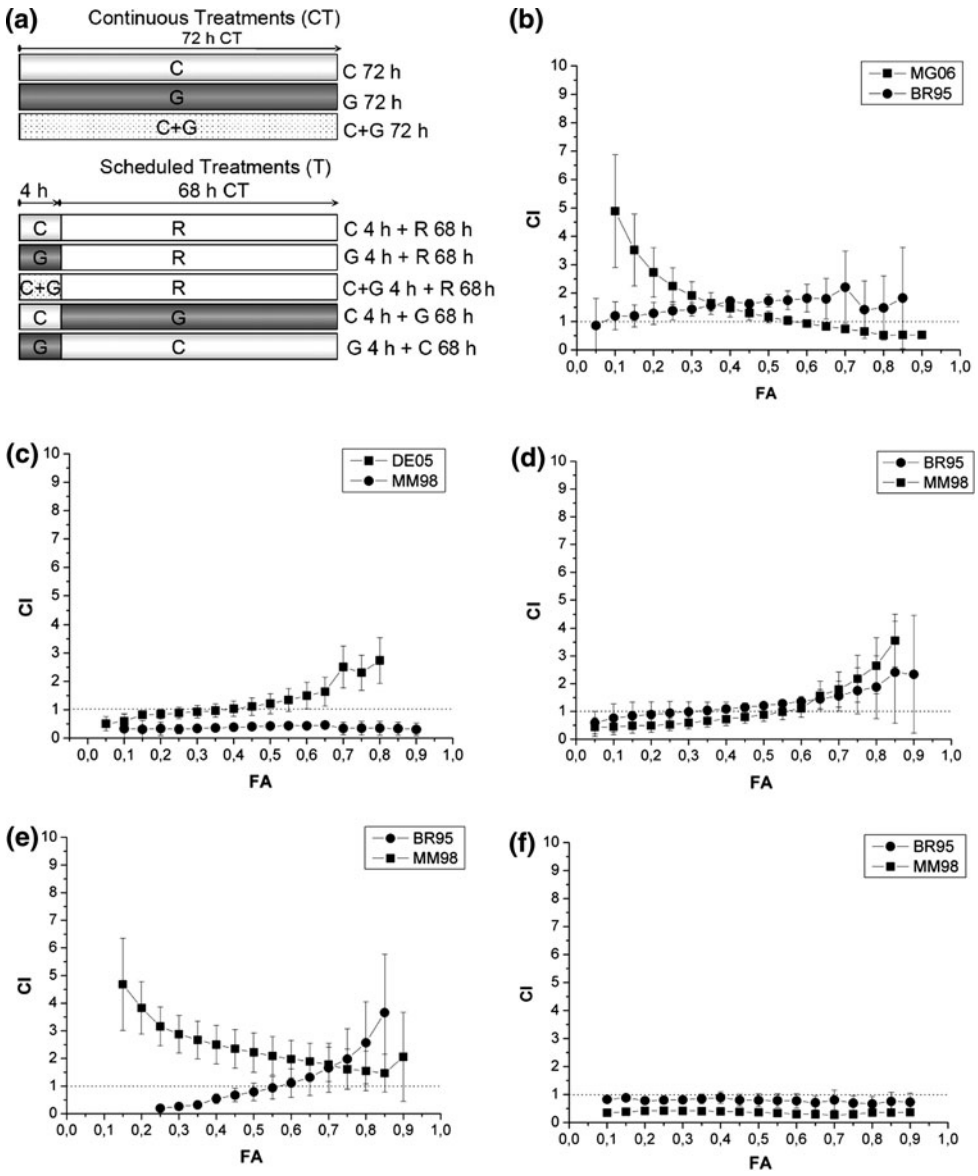

Fig. 1 Combination Index (CI) of cisplatin (*C*) and gemcitabine (*G*) for non-mutually exclusive drugs plotted against the fraction of affected cells (*FA*). **a** Scheme of drug treatments; **b** C and G were given simultaneously for 72 h to BR95 and MG06 (epithelioid); **c** C and G were given simultaneously for 72 h to the DE05 (mixed) and to MM98 (sarcomatous); **d** C and G were given simultaneously for 4 h T + 68 h R; **e** C was given for 4 + 68 h G; **f** G was given for 4 + 68 h

platin and/or gemcitabine according to the different schedules; at the end of drug treatment, cell lysates were prepared using an assay buffer containing 0.1 mM D-luciferin (Pierce), 2 μg/ml firefly luciferase (Sigma), 25 mM Tris pH 7.8, 5 mM $MgSO_4$, 100 μM EDTA, 1 mM NaN_3, 1 mM DTT, and 1% v/v Triton X-100; the light intensity was recorded using a ChemiDoc device (Bio-RAD).

Apoptotic cells were evaluated by in situ terminal deoxinucleotidyl transferase-mediated dUTP-biotin nick end labelling (TUNEL) assay. Briefly, cells were seeded onto glass slides (CultureSlides, BD Biosciences) at cell densities of 4×10^4 for BR95 and 2×10^4 for MM98), grown for 24 h, and subsequently treated for 4 h with gemcitabine at concentrations corresponding to the IC_{25} values obtained in each cell line, followed by cisplatin, again at cell-specific IC_{25}'s for further 20 or 44 h. At the end of the treatment, cells were fixed in 10% buffered formalin (pH 7.4) at RT for 25 min and washed twice in PBS. The TUNEL reaction was performed using the DeadEnd Colorimetric TUNEL System (Promega, Madison, WI), according to the manufacturer's instructions. Cell nuclei were counterstained with Mayer's haematoxylin; 8–10 fields were examined for each experimental condition.

Selection of cisplatin-resistant MPM cells

Selection of resistant cells was achieved by exposing 2×10^6 MM98 cells in a 10-mm Petri dish to a sublethal cisplatin concentration (1 μM); viable cells were subsequently re-plated onto a 25-cm^2 flask and grown in the presence of the same cisplatin concentration, replacing the medium twice a week, for a total of 6 months. After

about 2 months in this selective medium, the cells resumed growth and were expanded for further 4–6 months in order to obtain enough cells for IC_{50} measures and cryoconservation. At the end of the 6-month selection period, immunohistochemical reactions were performed with antibodies directed against a panel of mesothelial (calretinin, vimentin, cytokeratin 5/6, WT1, and HBME-1) and epithelial (carcinoembryonic antigen or CEA, BerEp4, CD15/Leu-M1, and TTF-1) markers [15], to verify whether the variant cells retained the phenotypic characteristic of the parental line. MM98 and MM98-R cells were seeded onto glass slides (CultureSlides, BD Biosciences), allowed to attach, and grown for 24 h, at the end of which they were fixed in 10% buffered formalin (pH 7.4) at RT for 25 min, followed by two washes in PBS. Fixed cells were treated with 3% hydrogen peroxide for 5 min, to abrogate endogenous peroxidase activity, and blocked with 1.5% horse serum for 20 min prior to incubation for 1 h at RT with primary mouse antibodies (Thermo Fisher Scientific, Fremont CA). The slides were then incubated with biotinylated goat anti-mouse IgG (Thermo Fisher Scientific, Fremont CA), followed by peroxidase-labelled streptavidin solution for 20 min at RT. Immunocomplexes were visualized using the peroxidase substrate 3,3′-diaminobenzidine (DAB); cell nuclei were counterstained with haematoxylin. For each staining, negative control slides were prepared by omitting primary antibodies.

Western blot

BR95 and MM98 cells were lysed in RIPA buffer (50 mM Tris–HCl, 150 mM NaCl, 1% Igepal CA-630, 0.1% SDS, pH 8) supplemented with protease inhibitor cocktail (Sigma) following 4 h or 72 h treatment with cisplatin at their respective IC_{50} values; cell debris was removed by centrifugation (30 min, 13,200 rpm, 4°C). Protein concentration in the supernatants was determined by the bicinchoninic acid method (BCA assay, Pierce Biotechnology, Celbio SpA, Milan, Italy); 30 μg of proteins were run on a 10% SDS–PAGE, blotted onto a polyvinylidene fluoride (PVDF) membrane (Immobilon-P, Millipore, MA, USA), blocked with 5% w/V non-fat milk and detected by anti-phospho-p53 primary antibody (9284, rabbit polyclonal Cell Signaling Technology, Celbio S.p.A., Milan, Italy). Lysates from the human squamous carcinoma cell line A431, expressing mutant p53 at high levels, were used as positive controls [16]. A peroxidase-conjugated anti-rabbit antibody was used to detect immunoreactive bands (Bethyl Laboratories Inc., Tema Ricerca, Bologna, Italy), and the corresponding chemiluminescence was determined by ECL (Immobilon Western, Millipore, MA, USA), using a ChemiDoc apparatus (Bio-Rad laboratories, Hercules, CA).

Cell cycle analysis

BR95 and MM98 cells were exposed to cisplatin and/or gemcitabine at their respective IC_{25} values, in order to avoid excessive cell mortality. After 72-h CT, they were washed with ice-cold PBS, recovered by trypsinization, fixed in 70% cold ethanol, and stored at −20°C. Before the analysis, the cells were washed in PBS, counted, resuspended at 10^6 cells/ml, and treated with 20 μg/ml RNAse A in PBS (for 30 min at room temperature), then they were further diluted to 10^5 cells/ml in PBS containing 50 μg/ml propidium iodide (PI). Flow cytometric analysis was performed with a Partec PAS IIIi instrument (Partec GmbH, Muenster, Germany), using a 488-nm laser as excitation source and the company recommended filter set up for detection (TK420 + EX488). The data were collected and analysed with the FloMax software.

Neutral comet assay

BR95 and MM98 were treated for 72 h at 37°C with cisplatin and/or gemcitabine at concentrations corresponding to their respective IC_{25} values, according to different schedules. Cells incubated in drug-free medium were used as negative controls (non-treated, NT). After 72 h drug treatment, the cells were washed with PBS and trypsinized. About 3×10^4 cells were suspended in 0.5% low melting point (LPM) agar, deposited on normal melting point (NMP) 1% agarose pre-coated microscope slides, and overlayed by another layer of 0.5% LMP agar. Each experiment was replicated three times. Cell lysis was carried out overnight at 4°C in 100 mM EDTA, 2.5 M sodium chloride, 0.5% *N*-lauroylsarcosine, 10 mM Tris base, 1% Triton™ X-100, and 10% DMSO. Alkali DNA unwinding (40 min) was performed in 0.5 M disodium EDTA, 300 mM NaOH, pH > 14; slides were neutralized by three washes in Tris–acetate 0.5 M pH 7.5. Electrophoresis was carried on TBE, pH 8, for 40 min at 25 V. Slides were washed in ice-cold 70% ethanol, and DNA was stained with Hoechst 33258 dye 0.2 μg/ml in PBS. Digital images of the nuclei were recorded using an Axiocam digital camera (Carl Zeiss, Inc., Thornwood, NY) mounted on a fluorescence microscope (Axiovert, also from Carl Zeiss, Inc.) at a 200× magnification ratio. The percentage of damaged nuclei was quantified by visual evaluation, performed independently by two researchers.

Data analysis and statistics

Cell viability data were normalized for the respective values obtained for untreated control cells (corresponding to 100%); IC_{50} (drug concentration inhibiting cell growth by 50%) values were extrapolated by sigmoidal curve fitting

using Origin 7 (Microcal). Each drug concentration or combination thereof was tested at least in triplicate, while the final data were calculated from three to nine replicates of the same experiment. FA values, defined as the fractions of cells affected by drug treatment, were used to calculate the corresponding-combination index (CI) values for non-mutually exclusive drugs [17]. CI values of approximately 1 indicate additive effects; values < 1 result from synergistic interactions, whereas antagonism is indicated for CI > 1.

For cell cycle analysis, changes in population distribution were assessed for statistical significance by the χ^2 test, using a spreadsheet editor. Other data were analysed using Student's *t* test (two tailed).

Results

IC_{50} values (Table 1) for cisplatin and gemcitabine were obtained using the MTS assay and were confirmed by means of the ATP chemosensitivity assay (not shown).

Different schedules can affect the outcome of cisplatin/gemcitabine combination therapy

Simultaneous exposure of MPM cells to cisplatin and gemcitabine for 72 h resulted in slight antagonism in epithelioid BR95 and MG06 cell lines (CI ≥ 1, Fig. 1b); in DE05 cells, (mixed phenotype) an additive trend was observed, whereas sarcomatoid MM98 showed a consistent and significant synergism (Fig. 1c). Short-term (4 h) simultaneous exposure to cisplatin and gemcitabine, followed by 68 h R in drug-free medium, yielded additive effects in both BR95 and MM98 cells (Fig. 1d). Exposure to cisplatin for 4 h followed by gemcitabine for 68 h resulted in a strong antagonistic effect on MM98 and a variable effect on BR95, from synergistic to antagonistic (for FA > 0.6) (Fig. 1e). On the other hand, 4-h exposure to gemcitabine followed by cisplatin for 68 h increased the potency of the combination, leading to a smooth synergism in BR95 and a strong synergism in MM98 (Fig. 1f); thus, gemcitabine followed by cisplatin exerted a neat synergistic effect in both the epithelioid and the sarcomatoid MPM cell lines.

To establish whether the effects of 4 h pre-treatment with gemcitabine followed by cisplatin were cytostatic rather than cytotoxic, induction of apoptosis was assessed in BR95 and MM98 at 24 and 48 h using a TUNEL-based assay. For both cell lines, visual inspection of treated cells evidenced a marked reduction in cell numbers, as well as the presence of apoptotic cells, as shown in Online resource 1 for the 48 h time point.

Table 1 IC_{50} values for cisplatin and gemcitabine, as single agents or in combination, in human mesothelioma cells (mean ± SD of *n* independent replicates)

Cell line	Drug	Treatment	IC_{50} ± SD	*n*
BR95	CDDP	4 h T + 68 h R	11.5 ± 2.9 μM	4
MM98	CDDP	4 h T + 68 h R	3.29 ± 1.6 μM	6
BR95	Gemcitabine	4 h T + 68 h R	322 ± 160 nM	4
MM98	Gemcitabine	4 h T + 68 h R	2.17 ± 0.22 μM	3
BR95	CDDP	72 h CT	3.04 ± 0.72 μM	6
MM98	CDDP	72 h CT	5.33 ± 0.88 μM	6
MG06	CDDP	72 h CT	15.1 ± 4.2 μM	5
DE05	CDDP	72 h CT	14.7 ± 2.6 μM	4
BR95	Gemcitabine	72 h CT	38 ± 1.26 nM	9
MM98	Gemcitabine	72 h CT	9.83 ± 3.16 nM	7
MG06	Gemcitabine	72 h CT	26.3 ± 17.3 nM	4
DE05	Gemcitabine	72 h CT	1.63 ± 0.69 μM	5

Cell cycle effects of cisplatin/gemcitabine simultaneous and sequential combinations

In order to investigate the possible relationship between cell cycle effects and the observed synergism between cisplatin (C) and gemcitabine (G), we decided to investigate cell cycle distribution following exposure to the two drugs according to the different schedules. Figure 2 reports cell cycle distributions for BR95 (a) and MM98 (b) cells; the histograms from which they have been calculated are reported as Online resource 2. A strong S-phase accumulation, associated with G2/M decrease, was observed for combination schedules yielding synergistic interactions, e.g. 72 h simultaneous exposure to cisplatin and gemcitabine in MM98 and gemcitabine 4 h T followed by cisplatin 68 h CT. Conversely, the G2/M fraction increased or remained unchanged for all the non-synergistic combinations. Cisplatin per se induced G2/M accumulation in both cell lines, except for MM98 with 4 h exposure. To investigate the role played by p53 in cisplatin-induced G2/M checkpoint activation [18], we assessed the levels of p53 phosphorylation on Ser15, a post-translational modification that has been related to p53 transcriptional activation in response to DNA damage [19], following exposure to cisplatin for 4 h, 4 h followed by 68-h recovery in drug-free medium and 72 h. MM98 showed a low-intensity band after 4-h exposure (Fig. 3a) that disappeared when the cells were allowed to recover (Fig. 3b) but increased following 72-h exposure to cisplatin. Thus, in MM98 p53 activation persisted only as long as cisplatin was present in the culture medium. Indeed, p53 degradation probably occurred during the recovery period in fresh medium following cisplatin treatment, which explains why the overall cell cycle profile was not significantly different from the control (Fig. 2b). In contrast, extracts form untreated BR95 exhibited an intense immunoreactive band at a lower molecular weight when

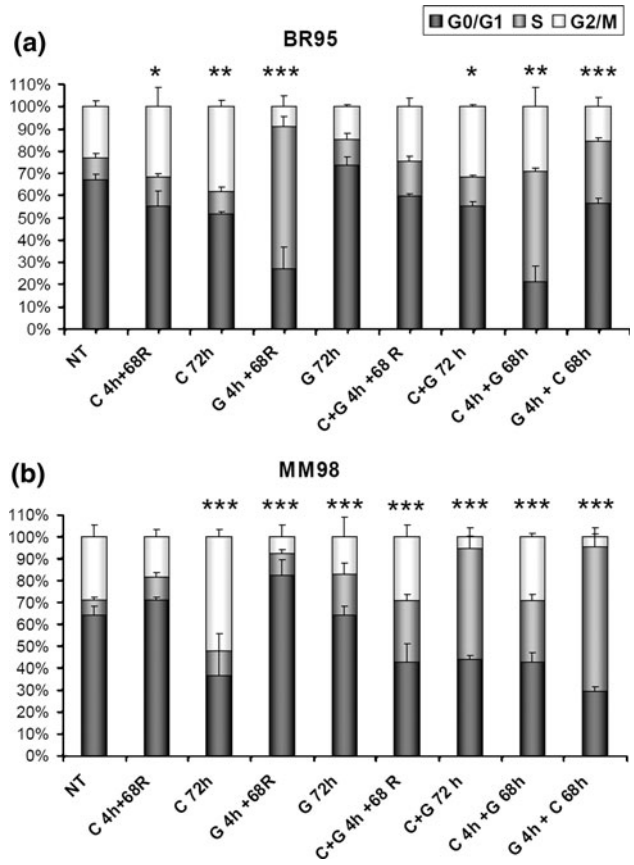

Fig. 2 Cell cycle distribution in BR95 (**a**) and MM98 (**b**) human MPM cell lines following treatment by cisplatin (C) and gemcitabine (G) or in combination at concentrations corresponding to their respective IC_{25} values. Results are the mean ± SD of three replicates and were compared to the control distribution (NT) by the χ^2 test (*$p < 0.05$, **$p < 0.01$, ***$p < 0.001$)

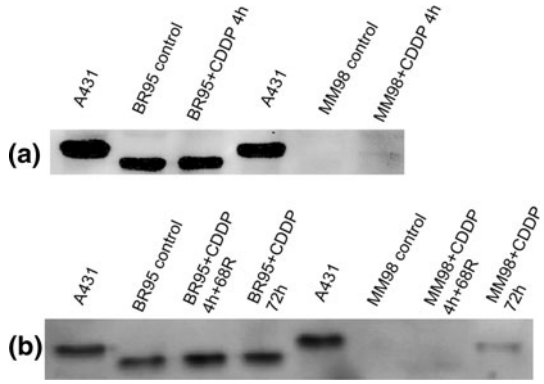

Fig. 3 Western Blot for phospho-p53. A431 lysate was used as positive control. **a** BR95 and MM98 were treated at their respective IC_{50} values for CDDP (obtained for 4 h + 68R treatments) and lysed after 4 h; **b** BR95 and MM98 were treated at their respective IC_{50} values (obtained for 4 h + 68R and 72 h treatments) for CDDP and lysed after 72 h

probed with antibodies for both the unphosphorylated (data not shown) and phosphorylated forms of p53, which was unaffected by cisplatin treatments (Fig. 3), suggesting the possibility that this cell line harbours a mutant form of the gene. Nevertheless, in BR95 the G2/M fraction also increased following cisplatin treatment, even though less markedly than in MM98, so possibly other proteins, such as p63 and p73, can replace p53 function after short-term treatment with cisplatin [20].

In cell cycle experiments, gemcitabine only induced S-phase accumulation in BR95 treated with the drug for 4 h, whereas both BR95 and MM98 mostly accumulated in the G0/G1 phase, which completely disrupted the cell cycle pattern (Online resource 2).

Pre-treatment with gemcitabine increases induction of double-strand breaks by cisplatin

During G2/M cell cycle arrest, DNA lesions can be proficiently repaired by homologous recombination (HR), whereas during the S phase they would preferably cause double-strand breaks (DSBs) following reparative DNA synthesis [21]. To detect DSBs following exposure to cisplatin and gemcitabine according to different schedules, we carried out a Neutral Comet Assay. As shown in Fig. 4, in MM98 cisplatin only induced DSBs after prolonged exposure, both as a single agent (72 h) and in combination with gemcitabine (gemcitabine 4 h T followed by cisplatin 68 h CT). In contrast, in BR95 a significant increase in DSBs was observed following cisplatin exposure for 4 and 72 h, both as a single agent and in the two combinations with gemcitabine yielding synergistic effects at low FA levels.

Effects of cisplatin/gemcitabine combinations on cisplatin-resistant MM98-R cells

MM98-R cells were obtained in our laboratory through continuous exposure (6 months) to a sublethal concentration of cisplatin. At the end of the selection period, the cells did not exhibit significant change in the typical mesothelial immunological profile that characterizes the parental cell line, i.e. they stained positively for the mesothelial marker calretinin, whereas they were negative for the epithelial markers Ber-Ep4 and CEA (Online resource 3). A slight decrease was only observed in vimentin (mesothelial marker) staining, possibly related to the morphological transition from a spindle to a polygonal shape, involving part of the cell population due to culture conditions. As shown in Fig. 5a, a 3.5-fold increase in IC_{50} for cisplatin following 72-h continuous exposure was observed in MM98-R cells when compared with MM98 ($p < 0.05$). On the contrary, MM98-R cells did not exhibit cross-resistance to gemcitabine (Fig. 5b).

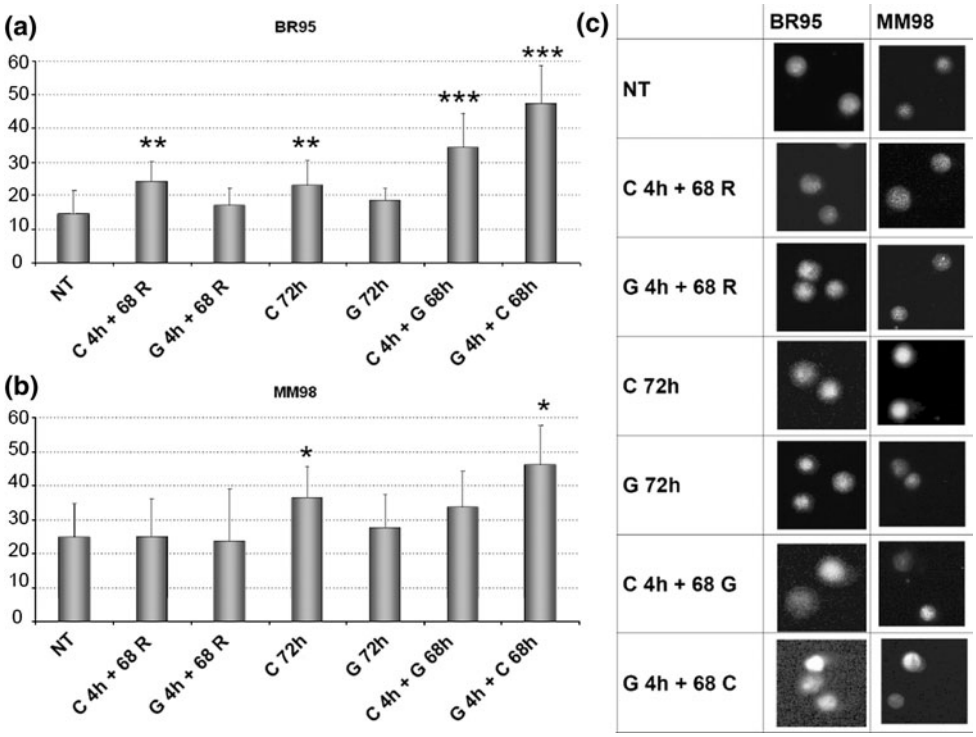

Fig. 4 Neutral Comet Assay following treatment by cisplatin (C), gemcitabine (G) or in combination at concentrations corresponding to their respective IC_{25} values. **a** Per cent of damaged BR95 nuclei after 72 h of treatment; **b** per cent of damaged MM98 nuclei after 72 h of treatment. Results are the mean ± SD of about 100 nuclei and were compared with the control (NT) by the two-tailed *t* test (*$p < 0.05$, **$p < 0.01$, ***$p < 0.001$). **c** Representative images of treated nuclei

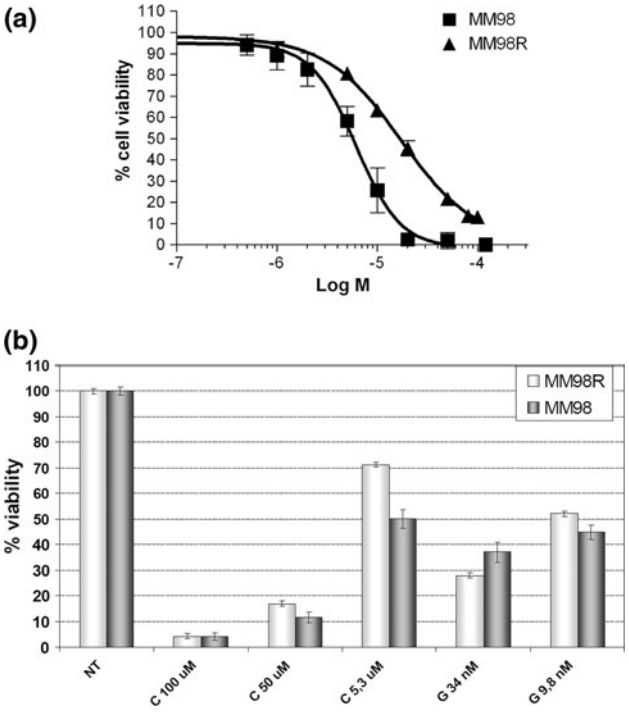

Fig. 5 **a** MM98 and MM98-R viability following 72 h CT with CDDP. Results are the means of three independent experiments. IC_{50} values were statistically different (two-tailed *t* test, $p < 0.05$). **b** MM98 versus MM98-R viability after 72 h treatment with cisplatin (C, 5.3, 50, and 100 μM, respectively, FA, 0.5, 0.7, and 1) and gemcitabine (G, 9,8 and 34 nM, respectively, FA 0.5 and 0.7). Results are the means of three independent experiments and were analysed by the two-tailed *t*-test: only MM98-R viability after 5.3 μM C treatment resulted significantly different ($p < 0.05$)

Discussion

The results of this study confirm clinical observations on MPM patients, indicating that cisplatin and gemcitabine exert synergistic effects in this disease [5, 6]. Importantly, our data highlight the impact of drug sequence on the outcome of cisplatin/gemcitabine treatments and identify pretreatment with gemcitabine followed by cisplatin as the most effective treatment schedule, in agreement with previous reports on a number of in vitro and preclinical in vivo models [7, 22].

Cisplatin is known to exert its cytotoxic activity mainly through formation of intra- and interstrand DNA-platinum adducts [23]. Gemcitabine, a cytidine analogue, acts by blocking nucleic acid synthesis, as well as several enzymes in the nucleotide biosynthesis pathway [24, 25], most notably ribonucleotide reductase, leading to a reduction in deoxynucleoside triphosphate (dNTP) pools, which contributes to inhibition of DNA synthesis and repair. As gemcitabine was found to increase adduct peak levels in ovarian carcinoma cell lines, by increasing adduct formation and by inhibiting their removal by the nucleotide excision repair (NER) system [26], we hypothesized that these effects might be involved in the cisplatin–gemcitabine synergism observed in MPM cell lines. Based on this hypothesis, our data could be explained as follows: when cisplatin exposure precedes gemcitabine, Pt–DNA adducts can be adequately repaired; in addition, a significant increase in dNTP pools has been demonstrated [27], which might antagonize the

effects of gemcitabine. On the other hand, when cells are exposed to gemcitabine before cisplatin, dNTP-depleted cells are able to remove intra- and inter-strand Pt-adducts but cannot fill the gaps created by the NER machinery, leading to single-strand (SSB)- and double-strand break (DSB) accumulation. DSBs are considered the most lethal DNA lesions, because they require HR to occur or they are repaired by non-homologous end joining, which can cause unsustainable genomic instability [28]. Knock-down of ERCC1 (an important component of the NER complex) has been shown to abrogate the cisplatin–gemcitabine synergism, and this effect has also been observed in HR-deficient cell lines [29, 30]. Actually, ERCC1 has been shown to act in both NER and HR, especially in the repair of interstrand cross-links [31] that may be caused by cisplatin. Since HR needs a sister chromatid, which is not produced until the end of the S phase, DNA lesions can only be proficiently repaired by HR during G2/M cell cycle arrest, whereas during the S phase reparative DNA synthesis would preferably cause DSBs [21]. DSBs were shown to be increased by cisplatin–gemcitabine combinations in ovarian AG6000 cells (variant of A2780 with induced resistance to gemcitabine), overexpressing ERCC1 [26, 27]. As previously reported in human anaplastic thyroid cancer cell lines [32], S-phase accumulation could account for the schedule-dependent synergistic effects we observed for the cisplatin–gemcitabine combination. In contrast, G2/M accumulation could facilitate DNA repair, thereby allowing cells to resume cell cycle progression [33]. Our results showed that in MPM cells, the additive-antagonistic effects were related to cisplatin-induced G2/M arrest, [34], possibly activating cellular damage response pathways, such as those depending on p53 or its homologues, whereby cell death by apoptosis can ensue.

In conclusion, our data indicate that schedule optimization can significantly increase the efficacy of a chemotherapy combination currently used in the clinical management of MPM. Thus, the present study could provide a solid background for the design of novel drug combinations also including targeted agents. Within this last class of anticancer agents, histone deacetylase inhibitors appear as a promising potential addition to cisplatin/gemcitabine combinations in MPM therapy, as they have been shown to enhance the antitumour effects of both DNA-damaging drugs, such as cisplatin [35], and antimetabolites, such as gemcitabine [36]. More specifically, valproate (a well-known antiepileptic drug recently shown to possess pan-HDAC inhibiting activity) has been found to increase the effects of the cisplatin/pemetrexed combination in mesothelioma cell lines and in tumour cells from patient's biopsies [37]. In addition, valproate is clinically well tolerated, has few side effects, and does not exhibit cross-resistance with cisplatin in MM98-R cells [38]; thus, it would represent an attractive choice for the design of polypharmacologic combinations to be tested on MPM cells. Further studies, combining the conventional two-dimensional approach on monolayer cultures with more realistic three-dimensional models [8], as well as the development of reliable animal models will be planned to test this hypothesis.

Acknowledgments We gratefully thank European Union (COST D39 action "Metallo-Drug Design and Action"), Regione Piemonte (CIPE project-code A 370 and Ricerca Sanitaria Finalizzata 2009), Associazione Sviluppo e Territorio (ATF, Alessandria) and "Metal in Life and Environment" Consortium (CIRCMSB, Bari) for financial support. Finally, we are indebted to the anonymous referees, whose criticisms and suggestions improved the quality of the manuscript.

References

1. Montanaro F, Rosato R, Gangemi M, Roberti S, Ricceri F, Merler E, Gennaro V, Romanelli A, Chellini E, Pascucci C, Musti M, Nicita C, Barbieri PG, Marinaccio A, Magnani C, Mirabelli D (2009) Survival of pleural malignant mesothelioma in Italy: a population-based study. Int J Cancer 124:201–207
2. Berghmans T, Paesmans M, Lalami Y, Louviaux I, Luce S, Mascaux C, Meert AP, Sculier JP (2002) Activity of chemotherapy and immunotherapy on malignant mesothelioma: a systematic review of the literature with meta-analysis. Lung Cancer 38:111–121
3. Kindler HL (2008) Systemic treatments for mesothelioma: standard and novel. Curr Treat Options Oncol 9:171–179
4. Green J, Dundar Y, Dodd S, Dickson R, Walley T (2007) Pemetrexed disodium in combination with cisplatin versus other cytotoxic agents or supportive care for the treatment of malignant pleural mesothelioma (Review). Cochrane Database Syst Rev 2:1–17
5. Kalmadi SR, Rankin C, Kraut MJ, Jacobs AD, Petrylak DP, Adelstein DJ, Keohan ML, Taub RN, Borden EC (2008) Gemcitabine and cisplatin in unresectable malignant mesothelioma of the pleura: a phase II study of the Southwest Oncology Group (SWOG 9810). Lung Cancer 60:259–263
6. Utkan G, Büyükçelik A, Yalçin B, Akbulut H, Demirkazik A, Dinçol D, Onur H, Gören D, Mousa U, Senler FC, Içli F (2006) Divided dose of cisplatin combined with gemcitabine in malignant mesothelioma. Lung Cancer 53:367–374
7. Bergman AM, Ruiz van Haperen VW, Veerman G, Kuiper CM, Peters GJ (1996) Synergistic interaction between cisplatin and gemcitabine in vitro. Clin Cancer Res 2:521–530
8. Padrón JM, van Moorsel CJ, Bergman AM, Smitskamp-Wilms E, van der Wilt CL, Peters GJ (1999) Selective cell kill of the combination of gemcitabine and cisplatin in multilayered postconfluent tumor cell cultures. Anticancer Drugs 10:445–452
9. Travis WD, Brambilla E, Muller-Hermelink HK, Harris CC (eds) (2004) World Health Organization Classification of Tumours. Pathology and genetics of tumours of the lung, pleura, thymus and heart. IARC Press, Lyon
10. Orecchia S, Schillaci F, Salvio M, Libener R, Betta PG (2004) Aberrant E-cadherin and gamma-catenin expression in malignant mesothelioma and its diagnostic and biological relevance. Lung Cancer 45S:S37–S43
11. Sigalotti L, Coral S, Altomonte M, Natali L, Gaudino G, Cacciotti P, Libener R, Colizzi F, Pianale G, Martini F, Tognon F, Jungbluth A, Cebon J, Maraskovsky E, Mutti L, Maio M (2002) Cancer testis antigens expression in mesothelioma. Br J Cancer 86:979–982
12. Toma S, Colucci L, Scarabelli L, Scaramuccia A, Emionite L, Betta PG, Mutti L (2002) Synergistic effect of the anti-HER-2/neu

antibody and cisplatin in immortalized and primary mesothelioma cell lines. J Cell Physiol 193:37–41
13. Mantel N (1958) An experimental design in combination chemotherapy. Ann NY Acad Sci 76:909–931
14. Sevin BU, Peng ZL, Perras JP, Ganjei P, Penalver M, Averette HE (1988) Application of an ATP-bioluminescence assay in human tumor chemosensitivity testing. Gynecol Oncol 31:191–204
15. Marchevsky AM (2008) Application of immunohistochemistry to the diagnosis of malignant mesothelioma. Arch Pathol Lab Med 132:397–401
16. Reiss M, Brash DE, Muñoz-Antonia T, Simon JA, Ziegler A, Vellucci VF, Zhou ZL (1992) Status of the p53 tumor suppressor gene in human squamous carcinoma cell lines. Oncol Res 4:349–357
17. Chou TC, Talalay P (1984) Quantitative analysis of dose-effect relationships: the combined effects of multiple drugs or enzyme inhibitors. Adv Enzyme Regul 22:27–55
18. Kastan MB, Onyekwere O, Sidransky D, Vogelstein B, Craig RW (1991) Participation of p53 protein in the cellular response to DNA damage. Cancer Res 51:6304–6311
19. Shieh SY, Ikeda M, Taya Y, Prives C (1997) DNA damage-induced phosphorylation of p53 alleviates inhibition by MDM2. Cell 91:325–334
20. Pietsch EC, Sykes SM, McMahon SB, Murphy ME (2008) The p53 family and programmed cell death. Oncogene 27:6507–6521
21. Budzowska M, Kanaar R (2009) Mechanisms of dealing with DNA damage-induced replication problems. Cell Biochem Biophys 53:17–31
22. van Moorsel CJ, Pinedo HM, Veerman G, Vermorken JB, Postmus PE, Peters GJ (1999) Scheduling of gemcitabine and cisplatin in Lewis lung tumour bearing mice. Eur J Cancer 35:808–814
23. Cepeda V, Fuertes MA, Castilla J, Alonso C, Quevedo C, Pérez JM (2007) Biochemical mechanisms of cisplatin cytotoxicity. Anticancer Agents Med Chem 7:3–18
24. Mini E, Nobili S, Caciagli B, Landini I, Mazzei T (2006) Cellular pharmacology of gemcitabine. Ann Oncol 17(Suppl 5):v7–v12
25. Heinemann V, Xu YZ, Chubb S, Sen A, Hertel LW, Grindey GB, Plunkett W (1990) Inhibition of ribonucleotide reduction in CCRF-CEM cells by 2′, 2′-difluorodeoxycytidine. Mol Pharmacol 38:567–572
26. Peters GJ, Van Moorsel CJ, Lakerveld B, Smid K, Noordhuis P, Comijn EC, Weaver D, Willey JC, Voorn D, Van der Vijgh WJ, Pinedo HM (2006) Effects of gemcitabine on *cis*-platinum-DNA adduct formation and repair in a panel of gemcitabine and cisplatin-sensitive or -resistant human ovarian cancer cell lines. Int J Oncol 28:237–244
27. van Moorsel CJ, Pinedo HM, Veerman G, Bergman AM, Kuiper CM, Vermorken JB, van der Vijgh WJ, Peters GJ (1999) Mechanisms of synergism between cisplatin and gemcitabine in ovarian and non-small-cell lung cancer cell lines. Br J Cancer 80:981–990
28. Karagiannis TC, El-Osta A (2004) Double-strand breaks: signaling pathways and repair mechanisms. Cell Mol Life Sci 61:2137–2147
29. Yang LY, Li L, Jiang H, Shen Y, Plunkett W (2000) Expression of ERCC1 antisense RNA abrogates gemcitabine-mediated cytotoxic synergism with cisplatin in human colon tumor cells defective in mismatch repair but proficient in nucleotide excision repair. Clin Cancer Res 6:773–781
30. Crul M, van Waardenburg RC, Bocxe S, van Eijndhoven MA, Pluim D, Beijnen JH, Schellens JH (2003) DNA repair mechanisms involved in gemcitabine cytotoxicity and in the interaction between gemcitabine and cisplatin. Biochem Pharmacol 65:275–282
31. Bergstralh DT, Sekelsky J (2008) Interstrand crosslink repair: can XPF-ERCC1 be let off the hook? Trends Genet 24:70–76
32. Voigt W, Bulankin A, Müller T, Schoeber C, Grothey A, Hoang-Vu C, Schmoll HJ (2000) Schedule dependent antagonism of gemcitabine and cisplatin in human anaplastic thyroid cancer cell lines. Clin Canc Res 6:2087–2093
33. Miyagawa K (2008) Clinical relevance of the homologous recombination machinery in cancer therapy. Cancer Sci 99:187–194
34. Sorenson CM, Eastman A (1988) Influence of *cis*-diamminedichloroplatinum(II) on DNA synthesis and cell cycle progression in excision repair proficient and deficient Chinese hamster ovary cells. Cancer Res 48:6703–6707
35. Ozaki K, Kishikawa F, Tanaka M, Sakamoto T, Tanimura S, Kohno M (2008) Histone deacetylase inhibitors enhance the chemosensitivity of tumor cells with cross-resistance to a wide range of DNA-damaging drugs. Cancer Sci 99:376–384
36. Donadelli M, Costanzo C, Beghelli S, Scupoli MT, Dandrea M, Bonora A, Piacentini P, Budillon A, Caraglia M, Scarpa A, Palmieri M (2007) Synergistic inhibition of pancreatic adenocarcinoma cell growth by trichostatin A and gemcitabine. Biochim Biophys Acta 1773:1095–1106
37. Vandermeers F, Hubert P, Delvenne P, Mascaux C, Grigoriu B, Burny A, Scherpereel A, Willems L (2009) Valproate, in combination with pemetrexed and cisplatin, provides additional efficacy to the treatment of malignant mesothelioma. Clin Cancer Res 8:2818–2828
38. Osella D et al. (in preparation)